

Tip–Sample Distance Dependence in the STM-Based Orbital-Mediated Tunneling Spectrum of Nickel(II) Tetraphenylporphyrin Deposited on Au(111)

Wenli Deng and K. W. Hipps*

Department of Chemistry and Materials Science Program, Washington State University,
Pullman, Washington 99164-4630

Received: April 6, 2003; In Final Form: July 23, 2003

Orbital-mediated tunneling spectra obtained in the STM environment are reported for nickel(II) tetraphenylporphyrin, NiTPP, as a function of molecule–tip separation. Spectra were acquired over a range of tip motion of 0.42 nm. Spectra did not show the variation in band splitting with tip distance predicted by several models. It appears for molecules such as NiTPP that the average potential at the molecule is essentially the same as at the metal substrate, at least for gap resistance values greater than 500 M Ω . Thus, at least for molecules of the height of NiTPP, the STM–OMT spectra should give reliable occupied and unoccupied orbital energies over a wide range of tip–molecule distances. An unexpected small shift of all orbital energies of NiTPP relative to the vacuum level is observed as a function of tip–molecule separation.

Introduction

Metalloporphyrins are intensively studied. They play an important role in biological processes such as oxygen transport and photosynthesis. They can act as catalysts¹ and can undergo reversible redox reactions in which the site of electron transfer may be localized on the porphyrin ring or on the central metal ion. Both reaction types are important in natural processes.² Recently, it has become known that structural distortions from planar geometry are fairly common and may also play a role in their solution phase chemistry.^{3–6} Thin porphyrin films on metal and semiconductor surfaces are also of great interest. Chemical sensors made from porphyrin films have been reported.⁷ Infrared (IR) spectroscopy,² Raman spectroscopy,⁸ and scanning tunneling microscopy (STM)^{9–15} studies have provided a wealth of information on the structure of porphyrins at the solution–electrode surface under controlled potential conditions. Langmuir–Blodgett films,¹⁶ self-assembled monolayers,^{9,17} and self-organized structures^{18,19} of porphyrins have been studied by a wide variety of techniques. Vapor-deposited porphyrins have received less attention.

Metal-free tetraphenylporphyrin (H₂TPP) thin films vapor-deposited onto KCl were studied by IR transmission spectroscopy and electron diffraction.²⁰ Ultrahigh-vacuum (UHV) studies of vapor-deposited Cu(II) tetrakis(3,5-di-*tert*-butyl-phenyl) porphyrin (CuTTBPP) on Cu(100) have been reported by Gimzewski,^{21,22} who has also provided an image of a mixed monolayer of CuTPP and CuTTBPP on Cu(100).²² Recently, Scudiero et al. reported a XPS, IR, STM, and STM–orbital-mediated tunneling (STM–OMT) studies of submonolayer films of CoTPP and NiTPP on Au(111) under UHV conditions.^{23,24} Scudiero et al. analyzed IR and XPS spectra of thin films of Co^{II}TPP, Cu^{II}TPP, and Ni^{II}TPP in terms of oxidation state, chemical composition, and orientation.²³ Molecular resolution STM images were reported, and chemical specificity in STM imaging for these complexes was demonstrated.^{23,24} As had been previously shown for metal phthalocyanine (MPc) complexes,^{25–27} varying the metal ion at the center of a metal(II) tetraphenylpor-

phyrin (MTPP) produced huge variations in the constant current STM images. This was interpreted as indicating large changes in tunneling probability associated with occupancy of the d_{z²} orbital of the transition metal ion. Scudiero et al. also provided electronic spectroscopic properties of metallotetraphenylporphyrins and nickel(II) octaethylporphyrin.^{24,28} In particular, they determined the energies of the highest occupied and lowest unoccupied π orbitals, and the highest occupied d metal orbital. For the first time, results from STM and tunnel diode-based orbital-mediated tunneling spectroscopy, and from ultraviolet photoemission spectroscopy (UPS) measurements on the same species were reported and compared. All three types of spectra were in agreement in their regions of overlap.^{24,28} An electrochemical model for estimating orbital-mediated tunneling bands was found to give good qualitative agreement with experiment, and good quantitative agreement for transient reduction processes and oxidative processes near the Fermi energy, E_F.

In all of these reports, STM-based orbital-mediated tunneling spectra, STM–OMTS were reported as if the observed transient oxidation and reduction bands were independent of tip–sample separation. The excellent agreement reported between the observed energies and those reported from UPS and electrochemistry justified the interpretations proposed but does not provide assurance that spectra taken at different set points (tip–sample separation) would provide identical results. The possibility that changing the distance between the tip and the molecular film might also change the OMT peak positions is raised by previous theoretical^{29–33} and experimental^{34–41} studies. For example, the tip–dot separation in STM studies of quantum dots plays a major role in the observed tunneling spectra.^{34,35} When the tip–dot distance is large such that the tip–dot impedance is greater than the dot–substrate impedance, the electronic affinity levels of the dot are measured. As the tip–dot distance shrinks such that the tunneling rate from tip to dot far exceeds that from the dot to the substrate, a coulomb blockade is observed and the apparent positions of the affinity levels shift. This apparent shift is due to the fact that the local potential at the dot is less than the potential applied between tip and substrate. The peripheral phenyl groups on tetraphen-

* Corresponding author. E-mail: hipps@wsu.edu.

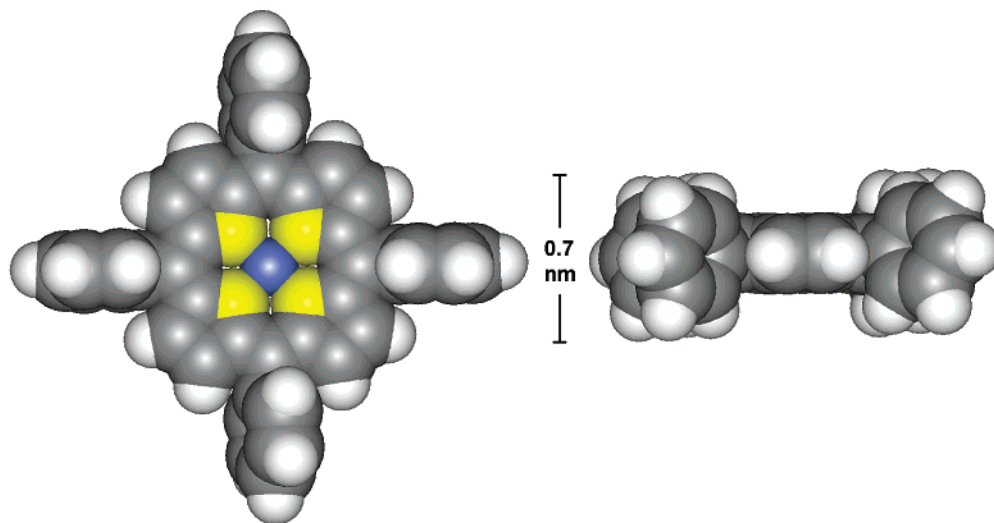


Figure 1. Space-filling model structure of NiTPP. The color code used is as follows: carbon is gray, hydrogen is white, nitrogen is yellow, and nickel is blue.

ylporphyrins might act as insulating spacers making the complex behave as a quantum dot. Tip-sample distance effects have also been seen in other materials. Distance dependent I - V curves obtained from CVD diamond films have been explained by tip field induced band bending at the semiconductor surface.³⁶ Scanning tunneling spectroscopy on the 6H-SiC(0001) (3×3) surface at large tip-sample distances exhibit distinct bands of empty and filled states.³⁸ However, the STS spectra become completely featureless in the range of small tip-surface distances and reveal a metallic-like Ohmic I - V dependence.

Even in the particular case of porphyrin complexes, there have been suggestions that the OMTS band positions might be dependent on the tip-molecule separation. For example, Schmickler²⁹ and Sumi³² have both proposed models for the tunneling process in which the local field at the porphyrin can be significantly different than the applied sample bias. As the tip-molecule distance increases, the observed peak positions should shift toward the values predicted from other techniques. Lindsay and co-workers³⁹ attempted to measure experimentally the ratio of local to applied potential, but were unable to demonstrate a significant difference.

In this paper, we will report an experimental study of the role of tip-sample separation on the OMTS obtained from a monolayer of nickel(II) tetraphenylporphyrin (NiTPP) vapor-deposited on Au(111) under ultrahigh vacuum (UHV) conditions. Adjusting the setpoint prior to spectral measurement controls the tip-sample distance. We will demonstrate that over a wide range of currents (a factor of 20) the OMTS is essentially independent of setpoint.

Experimental Section

Materials: Nickel(II) tetraphenylporphyrin [nickel(II) 5,10-,15,20-tetraphenyl-21*H*,23*H*-porphine, $C_{44}H_{28}N_4Ni$, NiTPP] was purchased from Porphyrin Products and used as supplied. A CPK model of the compound is shown in Figure 1. NiTPP was deposited from Ta metal sources in the same chamber as was used for the STM studies. Gold metal was purchased from Cerac and was of >99.999% purity.

STM Sample Preparation and Data Acquisition: Epitaxial Au(111) films with well-defined terraces and single atomic steps were prepared on mica by previously described methods.^{25,27} These films were about $0.15 \mu\text{m}$ thick and had a mean single grain diameter of about $0.5 \mu\text{m}$. Unlike true single-crystal gold,⁴²

these small crystal grains showed reconstruction line spacing ranging from 6.3 to about 9.0 nm. The gold films were transferred via air-lock into the UHV STM chamber (working pressure $\sim 6 \times 10^{-10}$ Torr) where NiTPP was deposited and then studied without exposure to air. The thickness of the NiTPP layer was determined with a quartz crystal thin film monitor. The deposition rates used were 0.01 nm/s, and the final film was about 1 monolayer. The STM head used was produced by McAllister Technical Services (Coeur d'Alene, ID) and is of the inertial approach type. A Digital Instruments Nanoscope III controller was used to acquire and process the reported data. Filtered, constant current images are reported. All images and spectra were acquired at about 20 °C. Both etched W and cut $Pt_{0.8}Ir_{0.2}$ tips were used. Generally, the tips required a UHV cleaning step (electron beam bombardment) in order to produce high quality images. Spectroscopy was performed by measuring both $I(V)$ and $dI/dV(V)$ as a function of V at fixed tip-sample separation (feed back off). The Digital Instruments software was used to collect both types of data simultaneously by utilizing an applied bias modulation of 100 mV. For reasons to be discussed later, these spectra were also transformed to $d(\ln I)/d(\ln V(V))$ form by dividing smoothed and interpolated dI/dV data by smoothed and interpolated I/V data. After a sequence of $dI/dV(V)$ and $I(V)$ curves were acquired, the current as a function of tip-sample separation, $I(z)$ was measured to provide a means of converting setpoint values to relative tip displacements. Typically, the spectroscopy data was acquired by first stabilizing the tip-sample height at a selected bias voltage and tunneling current. The feedback loop was opened and the modulated bias voltage was ramped from -2 to $+2$ V. During this ramp, $I(V)$ and $dI/dV(V)$ curves were acquired at 256 points with a dwell time of about 120 μs per point. The bias was then reset to the selected setpoint and the feedback loop was reestablished. In a similar manner, the $I(z)$ curves were collected by stepping the z voltage to the z piezoelectric element (increasing the distance beyond the setpoint value) with the feedback off and a dwell time of about 120 μs per point.

Results and Discussion

A typical medium resolution constant current image of NiTPP on Au(111), as observed in this study, is shown in Figure 2. Higher resolution images have been reported elsewhere.^{23,24,43,44} All the samples used for acquiring the reported spectra had a

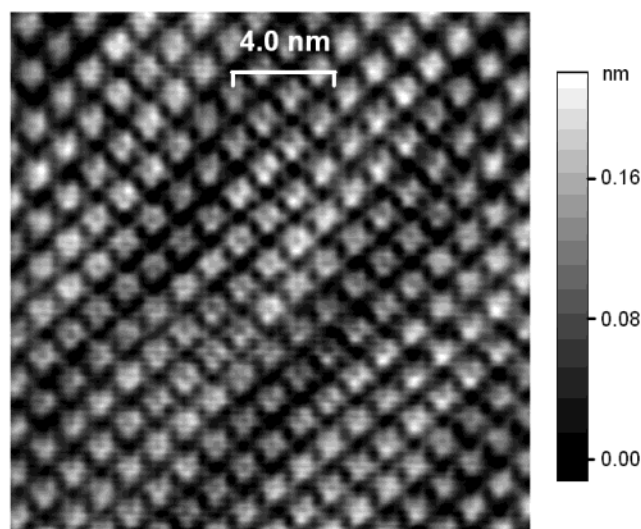


Figure 2. Constant current medium resolution STM image of a NiTPP monolayer on Au(111) under UHV conditions at room temperature. Sample bias voltage was -1.2 V, and the setpoint current was 0.390 nA.

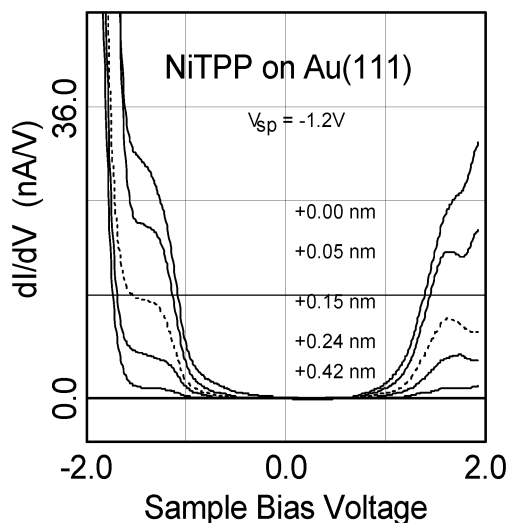


Figure 3. Orbital-mediated tunneling spectra (dI/dV curves) acquired from a NiTPP monolayer at -1.2 V sample bias and varying tip–substrate distance. Note that the distances given are increases in tip–substrate separation relative to the curve taken at closest approach (-1.2 V and 2.0 nA).

dense monolayer similar to the one shown in the figure. The apparent depression in the center of the molecule is associated with the filled d_{z^2} orbital of the Ni(II) ion—removal of one of these electrons does not occur at the bias voltage used to acquire this image.

Figure 3 presents the dI/dV curves obtained at differing tip–sample heights. The change in this distance, Δz , was set by changing the setpoint prior to measuring the dI/dV curve. The actual values of Δz were read off the $I(z)$ curves acquired during the same sessions, and with the same tips, as for the reported dI/dV spectra. The roughly 0.4 nm increase in Δz results from an approximate 20-fold decrease in setpoint current. Determining the peak positions and peak shapes from the presented data is extremely difficult because of the strong variation in both the resonant and elastic (background) intensities with tip–sample separation. Strosio and Feenstra^{45–47} considered this problem several years ago and determined that this difficulty could often be eliminated by using the logarithmic derivative, $d(\ln I)/d(\ln V(V))$, as the spectral intensity function. Later, Ukrainstev

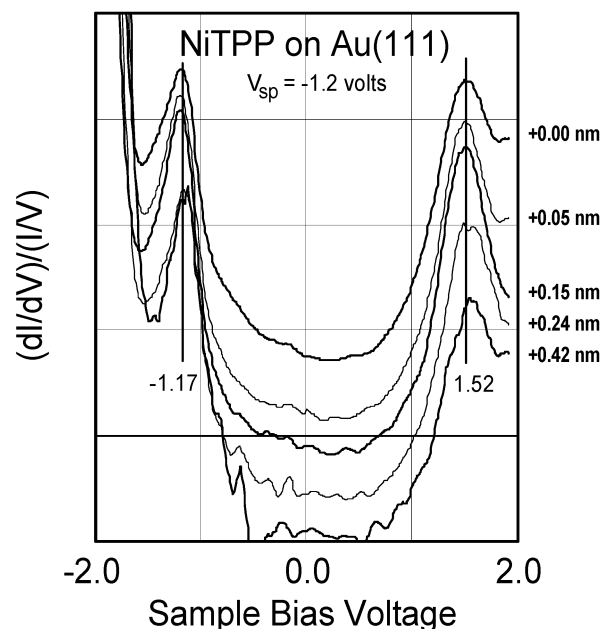


Figure 4. Logarithmic derivative, $d\ln I/d\ln V$, orbital-mediated tunneling spectra formed from the same data set as shown in Figure 3. Note that the distances given are increases in tip–substrate separation relative to the curve taken at closest approach (-1.2 V and 2.0 nA). A different constant was added to each data set to allow them to be better distinguished. All data sets went through zero at zero bias.

discussed some problems with this method in special cases.⁴⁸ In our case, we expect the Strosio and Feenstra method to work well.

Figure 4 is the STM–OMTS in the logarithmic derivative form based on the same data set displayed in Figure 3. A different constant was added to each data set to allow them to be better distinguished. All the original data sets went through zero at zero bias. As expected, it is now much easier to identify the peak positions and band shapes. Even the significant increase in noise associated with the low current measurements (~ 100 pA, $\Delta z = 0.42$ nm) is not sufficient to impede identification of the OMTS bands. The first transient reduction (electron affinity level) occurs 1.52 V above the Fermi energy while the first transient oxidation (ionization level) occurs about 1.17 V below the Fermi energy. Using a value of 5.20 eV for the Fermi energy,²⁴ one finds that relative to the vacuum level the highest occupied level lies near 6.37 eV and the lowest unoccupied level is near 3.68 eV. These values are in reasonable agreement with the values of 6.5 and 3.5 eV reported previously from UPS and dI/dV OMTS.²⁴

It is important to note that the splitting between the HOMO and LUMO OMTS bands does not change with tip–sample separation over a range of 0.42 nm. In the local field or quantum dot models, one would have expected the apparent separation to increase as the tip–molecule distance decreases. This is because only a portion of the bias voltage is the potential difference between tip and molecule (for electrons tunneling between the tip and the molecule) or between the Au and the molecule (for electrons tunneling between substrate and molecule). In the limit of equal and large tip–molecule and Au–molecule spacing, one would require twice the bias voltage necessary relative to the far-tip close-Au case. Moreover, the spectrum would be symmetrical in bias polarity.³⁶ Thus, the data presented in Figure 4 clearly demonstrate that the tip–molecule tunneling rate remains very much less than the molecule–Au tunneling rate throughout the 0.42 nm tip–molecule distance change.

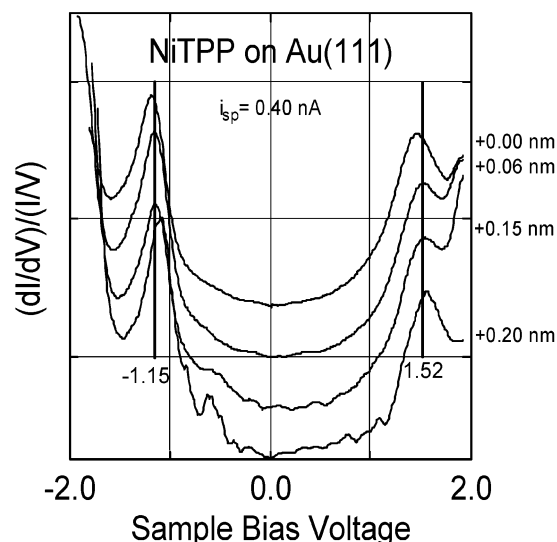


Figure 5. Orbital-mediated tunneling spectra obtained from a different sample and tip than reported in Figure 4. In this data set, the setpoint current was held constant and the applied bias was varied. A different constant was added to each data set to allow them to be better distinguished. All data sets went through zero at zero bias.

Nevertheless, there does appear to be a weak tip-sample distance effect that we did not expect. There is a small but persistent shift of the entire spectrum to lower energies relative to the Fermi energy as the tip moves closer to the surface. Both ionization and affinity peaks move deeper in energy by about 0.04 eV as the tip moves in by 0.42 nm. This shift is admittedly small with respect to the line widths, and might be an artifact of the data set used. To further investigate this issue, we collected a different type of data on a different sample with a different tip. Figure 5 shows the STM-OMTS obtained at fixed tunneling current but various values of setpoint voltage. These setpoint voltages were converted to Δz values by inverting experimental $I(z)$ curves. Despite the fact that the net tip motion is less for the data set in Figure 5, one still observes a small but definite trend. Moving the tip close to the molecule results in all the electronic orbitals being shifted down in energy.

An explanation for this may be that the increasing local field associated with close approach of the tip may induce increased interaction between molecule and substrate and/or increased polarization of the NiTPP. When the sample is biased positively, electron affinity states are observed. These negative ion states may be slightly stabilized by the polarization between tip and substrate. When the sample is biased negatively, positive ionization states are formed, and these may be less stable in this reversed polarity field. While we know of no identical examples in the literature, there are indications that high tip-induced fields can lead to significant energy level shifts. For example, Muller and co-workers measured work-function differences between tip and sample as a function of distance.⁴¹ For a Pt tip on a Au surface and for a W tip on a Pt surface, work-function differences of 0.2–0.6 eV were found. These differences increase with increasing distance and are smaller than expected. The work function difference at small distances seems to be much less than predicted from macroscopic work functions. Feenstra considered the measurement of electronic states of semiconductors by STM.⁴⁹ He concluded from theoretical calculations that tip-induced band bending due to the local high electric field between the tip and sample might result in spectral shifts of several tenths of an electronvolt. It is difficult to associate band bending with a layer only 1 molecule thick, but tip-field effects clearly can provide sufficient energy

to account for the magnitude of the shift observed here. We also caution that this effect may be one associated with NiTPP in particular rather than some universal phenomena.

One may ask why the expected band splitting and large shifts are not observed. Viewing the tunneling process as a sequential one with the molecule being an intermediate, one concludes that the tunneling rate between tip and molecule must be significantly smaller than that between Au substrate and the molecule. Given the exponential dependence of the tunneling current on distance, a simple explanation would be that even for the highest currents studied (a gap resistance of 600 M Ω) the molecule–Au resistance must be significantly less. For an ideal contact between molecule and Au, one would expect an impedance of only about 0.01 M Ω .⁵⁰ In the case of a xenon-metal contact this resistance has been calculated to be about 0.1 M Ω .⁵¹ Thus, even if the Au–molecule resistance was one or 2 orders of magnitude greater than for the Xe–metal case the Au–molecule tunneling rate would still be more than 100 times greater than the molecule–tip rate.

An alternative approach would be to ask what fraction of the total bias voltage is dropped across the molecule–tip gap. While simple electrostatic models are of limited value on this distance scale, they may provide qualitative insights. If one imagines the potential dropping uniformly between tip and metal substrate, the local field at the molecule would be determined by the ratio of the median height of the molecule to the substrate–tip distance. In the case of NiTPP, this distance is about 0.3 nm (see Figure 1), and we take the molecule–tip distance at closest approach to be given by the parameter t . Thus, one expects that (in this very crude model) the effective potential of the molecule relative to the tip would be

$$V(z) = \left[1 - \frac{0.3}{z}\right]V \quad (1)$$

Thus, the relative variation in the apparent resonance peaks would be given by

$$\Delta V/V = \left[\frac{0.3}{t(t + \Delta z)}\right]\Delta z \quad (2)$$

Assuming that $\Delta V/V$ is less than 0.05, and that Δz is 0.42 nm, t must be at least 1.0 nm. While this value does not at first appear unreasonable, it does pose a problem. If $t = 1$ is substituted into eq 1, the local potential is found to be only 70% of the applied bias. Given the excellent agreement between STM-OMTS peaks and the UPS and reduction potential data,²⁴ the local field cannot vary from the applied bias by more than about 5%. Thus, there is an obvious inconsistency. When we began this classical analysis, we agreed that it was at most of qualitative value. Recent theoretical calculations of conduction in molecular wires indicate a wide range of possibilities, from the entire potential drop occurring along the length of the molecule^{52–54} to constant potential across the molecular wire.^{55,56} Thus, it should not surprise us to find that simple electrostatic models do not work and that the local potential at the molecule is much closer to that of the substrate than the simple electrostatic model predicts.

This result is in fact very encouraging to those wishing to apply STM-OMTS to the analysis of the orbital energies of larger molecules. The size range of molecules that may be accurately studied with tip–substrate distances that give reasonable signal-to-noise ratios may be much larger than expected from simple electrostatic models. We plan to systematically study porphyrins with a range of progressively larger substituents

(and therefore greater Au–molecule separation) in order to experimentally determine at what distance between molecule and substrate it becomes impossible to neglect the role of tip–molecule separation in the observed spectra. While the similarity of W and Pt/Ir tip spectra observed to date suggests that the local work function of the tip is not playing a significant role in the observed spectra,²⁴ it will be useful to further verify this by using other tip materials, such as Au.

Conclusions

Changes in tip–sample distance over several angstroms and a factor of 20 in setpoint current produce no measurable changes in orbital energy splitting. This means that ionization and affinity level spectra obtained by STM–OMTS for molecules of the order of the size of porphyrins can be used reliably. It is further suggested that it may be possible to reliably measure STM–OMTS on molecules larger than tetraphenylporphyrin without concern about the tip–molecule separation distance, provided that the effective gap impedance does not drop below about 500 M Ω . At some as yet undetermined point, molecular size increases should lead to OMTS band positions that are tip–molecule distance dependent. An unexpected result of this study was the small but persistent shift of all OMTS bands to energies deeper than the vacuum level. In the case of NiTPP, this shift is of the order of 50 mV and may be associated with the electronic and structural properties of NiTPP rather than some universal phenomena.

Acknowledgment. We thank the National Science foundation for support in the form of Grants CHE 0138409 and CHE 0234726. Acknowledgment also is made to the donors of the Petroleum Research Fund, administered by the American Chemical Society.

References and Notes

- (1) Collman, J. P.; Halbert, T. R.; Suslick, K. S. *Metal Ions in Biology*; Spiro, T. G., Ed.; Wiley: New York, 1980; Vol. 2 p 1.
- (2) Jones, D.; Hinman, A. S. *J. Chem. Soc., Dalton Trans.* **1992**, 1503.
- (3) Unger, E.; Beck, M.; Lipski, R.; Dreybott, W.; Medforth, C. J.; Smith, K.; Schweitzer-Stenner, R. *J. Phys. Chem. B* **1999**, 103, 10022.
- (4) Pendergast, K.; Spiro, T. G. *J. Am. Chem. Soc.* **1992**, 114, 3793–3901.
- (5) Piffat, C.; Melamed, D.; Spiro, G. *J. Phys. Chem.* **1993**, 97, 7441.
- (6) Jentzen, W.; Unger, E.; Song, X.; Jia, S.; Tyek, I. T.; Stenner, R. S.; Draybrodt, W.; Scheidt, W. R.; Shelnutt, J. A. *J. Phys. Chem. A* **1997**, 101, 5789.
- (7) Paolesse, R.; Di Natale, C.; Dall'Orto, V.; Macagnano, A.; Angelaccio, A.; Motta, N.; Sgarlata, A.; Hurst, J.; Rezzano, I.; Mascini, M.; D'Amico, A. *Thin Solid Films* **1999**, 354, 245.
- (8) Atamian, M.; Donohoe, R. J.; Lindsey, J. S.; Bocian, D. F. *J. Phys. Chem.* **1989**, 93, 2236.
- (9) Duong, B.; Arechabaleta, R.; Tao, N. J. *J. Electroanal. Chem.* **1998**, 447, 63.
- (10) Kunitake, M.; Batina, N.; Itaya, K. *Langmuir* **1995**, 11, 2337.
- (11) Ogaki, K.; Batina, N.; Kunitake, M.; Itaya, K. *J. Phys. Chem.* **1996**, 100, 7185.
- (12) Kunitake, M.; Akiba, U.; Batina, N.; Itaya, K. *Langmuir* **1997**, 13, 1607.
- (13) Han, W.; Durantini, E. N.; Moore, T. A.; Moore, A. L.; Gust, D.; Rez, P.; Letherman, G.; Seely, G.; Tao, N.; Lindsay, S. M. *J. Phys. Chem. B* **1997**, 101, 10719.
- (14) Tao, N. J. *Phys. Rev. Lett.* **1996**, 76, 4066.
- (15) Tao, N. J.; Cardenas, G.; Cunha, F.; Shi, Z. *Langmuir* **1995**, 11, 4445.
- (16) Palacin, S.; Ruau-del-Teixier, A.; Barraud, A. *J. Phys. Chem.* **1986**, 90, 6237.
- (17) Shimazu, K.; Takechi, M.; Fugii, H.; Suzuki, M.; Saiki, H.; Yoshimura, T.; Uosaki, K. *Thin Solid Films* **1996**, 273, 250.
- (18) Thomas, P.; Berovic, N.; Laitenberger, P.; Palmer, R.; Bampos, N.; Sanders, J. *Chem. Phys. Lett.* **1998**, 294, 229.
- (19) Furukawa, M.; Tanaka, H.; Sugiura, K.; Sakata, Y.; Kawai, T. *Surf. Sci.* **2000**, 445, L58.
- (20) Yangi, H.; Ashida, M.; Harima, Y.; Yamashita, K. *Chem. Lett.* **1990**, 385.
- (21) Jung, T. A.; Schlittler, R. R.; Gimzewski, J. K.; Tang, H.; Joachim, C. *Science* **1996**, 271, 181.
- (22) Gimzewski, J. K.; Jung, T. A.; Cuberes, M. T.; Schlittler, R. R. *Surf. Sci.* **1997**, 386, 101.
- (23) Scudiero, L.; Barlow, D. E.; Hipps, K. W. *J. Phys. Chem. B* **2000**, 104, 11899.
- (24) Scudiero, L.; Barlow, D. E.; Mazur, U.; Hipps, K. W. *J. Am. Chem. Soc.* **2001**, 123, 4073.
- (25) Lu, X.; Hipps, K. W. *J. Phys. Chem. B* **1997**, 101, 5391.
- (26) Lu, X.; Hipps, K. W.; Wang, X. D.; Mazur, U. *J. Am. Chem. Soc.* **1996**, 118, 7197.
- (27) Barlow, D.; Hipps, K. W. *J. Phys. Chem. B* **2000**, 104, 2444.
- (28) Scudiero, L.; Barlow, D. E.; Hipps, K. W. *J. Phys. Chem. B* **2002**, 106, 996.
- (29) Schmickler, W., J. *Electroanal. Chem.* **1990**, 296, 283.
- (30) Onipko, A. I.; Berggren, K.-F.; Klymenko, Yu. O.; Malysheva, L. I.; Rosink, J. J. W. M.; Geerligs, L. J.; van der Drift, E.; Radelaar, S. *Phys. Rev. B: Condens. Matter Mater. Phys.* **2000**, 61, 11118.
- (31) Plihal, M.; Gadzuk, J. W. *Phys. Rev. B: Condens. Matter Mater. Phys.* **2001**, 63, 085404/1.
- (32) Sumi, H. *J. Phys. Chem. B* **1998**, 102, 1833.
- (33) Zhang, J.; Chi, Q.; Kuznetsov, A. M.; Hansen, A.; Wackerbarth, H.; Christensen, H. E.; Andersen, J.; Ulstrup, J. *J. Phys. Chem. B* **2002**, 106, 1131.
- (34) Bakkers, E. P.; Hens, Z.; Kouwenhoven, L. P.; Gurevich, L.; Vanmaekelbergh, D. *Nanotechnology* **2002**, 13, 258.
- (35) Katz, D.; Millo, O.; Kan, S.; Banin, U. *Appl. Phys. Lett.* **2001**, 79, 117.
- (36) Snyder, S. R.; White, H. S. *J. Electroanal. Chem.* **1995**, 394, 177.
- (37) Cannaerts, M.; Nesladek, M.; Haenen, K.; De Schepper, L.; Stals, L. M.; Van Haesendonck, C. *Diamond Relat. Mater.* **2002**, 11, 212.
- (38) Gasparov, V.; Riehl-Chudoba, M.; Schroter, M.; Richter, W. *Europhys. Lett.* **2000**, 51, 527.
- (39) Han, W.; Durantini, E. N.; Moore, T. A.; Moore, A. L.; Gust, D.; Rez, P.; Letherman, G.; Seely, G.; Tao, N.; Lindsay, S. M. *J. Phys. Chem. B* **1997**, 101, 10719.
- (40) Klusek, Z. *Electron Technol.* **2000**, 33, 344.
- (41) Muller, A.-D.; Muller, F.; Hietschold, M. *Appl. Phys. Lett.* **1999**, 74, 2963.
- (42) Barth, J. V.; Brune, H.; Ertl, G.; Behm, R. J. *Phys. Rev. B* **1990**, 42, 9307.
- (43) Hipps, K. W.; Scudiero, L.; Barlow, D. E.; Cooke, M. P. *J. Am. Chem. Soc.* **2002**, 124, 2126.
- (44) Hipps, K. W.; Scudiero, L.; Barlow, D. E. *J. Phys. Chem. B* **2003**, 107, 2903.
- (45) Strosio J. A.; Feenstra R. M.; Fein A. P. *Phys. Rev. Lett.* **1986**, 57, 2579.
- (46) Feenstra R. M. *Phys. Rev. B* **1994**, 50, 4561.
- (47) Strosio J. A.; Feenstra R. M.; *Scanning Tunneling Microscopy*; Strosio J. A., Kaiser W. J., Eds.; Methods in Experimental Physics 27; Academic: New York, 1993.
- (48) Ukraintsev V. A. *Phys. Rev. B* **1996**, 53, 11176.
- (49) Feenstra R. M., *Phys. Rev. B* **1994**, 50, 4561.
- (50) Landauer, R. Z. *Phys. B* **1987**, 68, 217.
- (51) Yazdani, A.; Eigler, D. M.; Lang, N. D. *Science* **1996**, 272, 1921.
- (52) Datta, S.; Tian, W.; Hong, S.; Reifenberger, R.; Henderson, J.; Kubiak, C. P. *Phys. Rev. Lett.* **1997**, 79, 2530.
- (53) Tian, W.; Datta, S.; Hong, S.; Reifenberger, R.; Henderson, J.; Kubiak, C. J. *Chem. Phys.* **1998**, 109, 2874.
- (54) Mujica, V.; Roitberg, A.; Ratner, M. J. *Chem. Phys.* **2000**, 112, 6834.
- (55) Damle, P. S.; Ghosh, A.; Datta, S. *Phys. Rev. B* **2001**, 64, 201403.
- (56) Nitzan, A.; Galperin, M.; Ingold, G.; Grabert, H. *J. Chem. Phys.* **2002**, 117, 10837.